**SOLIDIFICATION PROCESSES AND MICROSTRUCTURES** *Edited by M. Rappaz, C. Beckermann and R. Trivedi*
***TMS (The Minerals, Metals & Materials Society), 2004***

# Characteristic Substructure in directionally solidified dilute Al-Cu Alloys

Osvaldo Fornaro[1], Hugo A. Palacio[2], Heraldo Biloni[2]

IFIMAT: Instituto de Física de Materiales Tandil
Universidad Nacional del Centro de la Provincia de Buenos Aires
Pinto 399 (B7000GHG) Tandil - Argentina
[1]Consejo Nacional de Investigaciones Científicas y Técnicas
[2]Comisión de Investigaciones Científicas de la Provincia de Buenos Aires

Keywords: Directional solidification, morphological stability, microsegregation

**Abstract**

Al-0.2 wt.% Cu alloy samples were directionally solidified under similar thermal gradient conditions. As the growth velocity was increased, the transition among successive stages from planar, nodes, bidimensional cells, regular cells and irregular cells was characterized through careful metallographic analysis of the microsegregation. During the different transitions, a nodal precipitation mechanism seems to be responsible for the evolution of the substructure, where the eutectic precipitation at the nodes plays a fundamental role in the fixation of the substructure. During planar to bands transition, the nodes slow down the interface at certain critical points of it, and the primary spacing can be well defined. This phenomenon seems to be similar during the transition of all the substructure stages under study. The primary spacing $\lambda_1$ fits the order of magnitude of maximum rate wavelength predicted by Morphological stability theory. In several cases, a second order microsegregation pattern at cellular wall level has been observed. This seems to be due to small variation in the microsegregation during the lateral growth of the cells in an enriched intercellular liquid. The secondary microsegregation pattern detected has a small periodicity $\lambda_{min}$ close to the minimum unstable wavelength predicted by the Morphological stability theory.

## Introduction

During the process of directional solidification of dilute alloys, the morphological stability theory [1–3] defines the conditions under which a planar solid liquid (S-L) interface becomes unstable. According to this theory, at low and moderate solidification rates, Modified Constitutional Supercooling (MCS) criteria can be applied [4]. Under a qualitative point of view, the decrease of the parameter $(G_L/VC_0)$, where $G_L$ is the thermal gradient in the liquid in front of the S-L interface, $V$ the solidification rate, and $C_0$ the nominal composition of the alloy, controls the evolution of the S-L interface from planar to arrayed dendritic.

Extensive research has been done on this subject both in organic transparent alloys and in metallic dilute alloys. In the latter case, different morphological stages [5] may be defined from planar S-L interface, nodes or depressions at the S-L interface, elongated or bi-dimensional cells, regular or hexagonal cells, distorted or branched cells, and dendritic cells or arrayed dendrites. The current knowledge is unclear in connection with the mechanism involved in the evolution of the different stages. In the literature only some concepts exist such as a node mechanism [5, 6], different expressions for the transition from cellular to dendritic growth [7–9] and theoretical works concerned with the apparition of nodes, cells and dendrites without discussion of the transition among them [10, 11]. The segregation details of the intercellular solute distribution were analyzed only partially. Then, we consider that a more carefully metallographic analysis in dilute Al-Cu alloys directionally grown may enlighten two important areas of knowledge: i) the microsegregation pattern of directional grown samples with different operational conditions; and ii) the possible mechanisms associated with the transitions among substructure stages above mentioned, using an experimental strategy based on the characterization of the solidification substructures.

The fundamental aim of this work is to evaluate the details of the microsegregation substructure and, eventually, to obtain a relationship between the pattern and the morphological evolution of the substructure during the directional solidification in dilute Al0.2wt.%Cu alloys, presenting substructures from nodes to irregular cells, using proper metallographic techniques to detect the details of the segregation substructure.

## Experimental

Directional solidification of Al-0.2wt.%Cu was carried out. The details of alloy preparation, growth of the samples, control of thermal and S-L interface velocity variables $(G_L/VC_0)$ and quenched of the S-L interface during the growth were previously published [12–14]. Also, some samples were grown for several centimeters long, typically 10 cm, without quenching the interface to verify if the observations were artifacts of quenching.

The analysis of the microstructure requires great attention on the sample preparation. The microstructure was observed both in longitudinal views (in growth direction) and cross sections. The surface was set up by mechanical polishing with grid 600 and then with a suspension of $6$ to $1\,\mu$m diamond powder with alcohol. Posterior electrolytical polishing using **e1** electrolyte defined in Table 1, gives us an adequate surface in order to obtain a good contrast at high magnification. To reveal and emphasize the microstructure, the solution **e2** of the same Table was used. This solution affects selectively rich cooper zones, such as Al-Cu eutectics or solute rich zones with different relieves. It was diluted at $33\%$ to slow down the reaction in some cases.

| | | | |
|---|---|---|---|
| **e1:** | 2-butoxy-ethanol | 80 ml | 33V |
| | glycerine | 10 ml | Al cathode |
| | $HClO_4$ | 10 ml | 15-60 s |
| **e2:** | dist. $H_2O$ | 190 ml | 20 s |
| | HCl | 20 ml | room temp. |
| | HNO | 5 ml | |
| | HF | 2 ml | |

Table 1: Metallographic settings

## Results and Discussion

Fig. 1 shows several typical microstructures corresponding to segregated cellular walls, showing different aspects of the observed patterns. Fig. 1 a) and b) corresponds to details on cellular growth. In order to disregard the presumption that the metallographically observed segregation pattern could be promoted by rapid final solidification of liquid during the S-L interface quenching, the microstructure was observed at different distances from the quenched interface as well as in samples grown by several cm long, typically 10 cm and obtained without the S-L interface quenching process. Both figures show a quite similar micro-segregated pattern in sample with and without quenching. It is clear that the lateral instabilities is a general phenomenon that may be interpreted as existent during the solidification process.

Once the characteristic distances were measured, two kinds of spacing arise: a primary spacing $\lambda_1$, corresponding to the distance among eutectic nodes, with a value between 150 to 300 $\mu$m with a dispersion of $\pm$ 4%, and a smaller segregated perturbation of the structure at the walls, which

b) c)

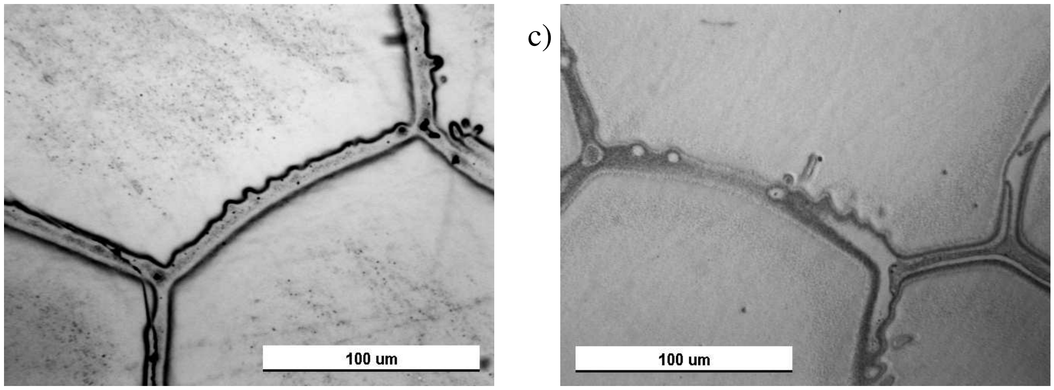


Figure 1: Lateral perturbations in cellular growth. Samples grown at $G_L = 25$ K/cm. a) $V = 12$ $\mu$m/s; at 2.5 mm far from the interface quenched; b) $V = 13$ $\mu$m/s; samples without quench.

we called $\lambda_{min}$ with a range between 15 to 25 $\mu$m with $\pm$ 8% typical dispersion, which has a smooth dependence on the growth velocity similar to the relation between $\lambda_1$ and $V$. We found that the relationship between both kinds of perturbations as $\frac{\lambda_1}{\lambda_{min}} \approx 12$ is in the range of velocities studied in this work.

To analyze the microstructure, we use concepts of Morphologycal Stability Theory. In this theory, a planar unstable front can evolve to a different morphology, trapping solute in the intercellular space during the process. The involved mechanisms in the spacing selection are in discussion, altough the fact that the fundamental growth morphology can be derived from the morphological stability theory [3] is broadly accepted. This theory assumes that if an initially planar front growing in $z$ direction advancing at velocity $V$ is perturbed with a spatial-time function $z = \delta \exp\left(\sigma t + \mathbf{i}\, 2\frac{\pi x}{\lambda}\right)$ where $\delta$ is the perturbation amplitude, $\lambda$ is the wavelength, the growth rate of the perturbation $\sigma$ could be determined under the frame of linear theory for small values of $\delta$ [5]. The solution for $\sigma$ is a function which includes the contribution of thermal, diffusive and capillary fields. Negative values of $\sigma$ for a given $\lambda$ value means that the planar front is stable to that kind of perturbations, while positive values mean an unstable condition.

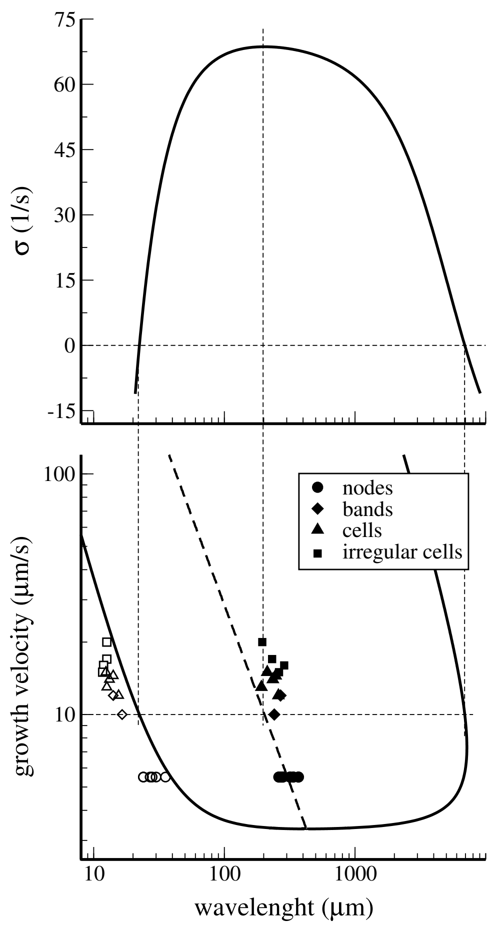


Figure 2: a) rate of perturbations at $V$ =10 $\mu$m/s and b) resulting stability map for Al-0.2 wt. %Cu, $G_L$ =25 K/cm.

For a given growth velocity, between $V_C$ (Modified Constitutional Supercooling) and $V_{abs}$ (Absolute stability criterium), $\sigma$ is positive for a range of wavelengths [5, 15]. The points where $\sigma = 0$ define the marginal stability condition for two different wavelengths $\lambda_0^{\pm}$. The marginal stability limits a zone where the planar growth will be unstable, with a maximum $\sigma$ for an intermediate wavelength $\lambda_{\sigma_M}$. Fig. 2 a) shows the solution of $\sigma$ calculated for an Al-0.2 wt% Cu alloy growing at $V = 10^{-3}$ cm/s, and and Fig. 2 b) the low velocity zone of the stability map, following the proposal of Coriell and Boettinger

[1994] in [5].

Under the view of this theory, unstable growths would have a primary spacing determined by a contribution of a set of wavelengths, each with different weights. Discussion is open about how these weighed wavelengths could contribute to the final spacing, but wavelengths close to $\lambda_{\sigma_M}$ have greater probability to contribute to the primary spacing [3, 16].

This fact could be seen superimposing experimental measured spacings obtained for nodes, bands, regular and irregular cells on a stability map obtained for $G_L = 25$ K/cm and $C_0$= 0.2wt.%Cu [5]. Fig. 2 shows that experimental $\lambda_1$ is found on the central part of unstable zone, close to the maximum rate's wavelength. Similar results were obtained by Cheveigné *et al.* [17] in succinonitrile-acetone. Also, Cheveigné *et al.* reviewed experimental results from different authors in metallic alloys with a similar tendency [18]. More recently, numerical predictions in a 2D symmetry for intermediate and rapid growth velocity presented by Boettinger and Warren [19] give the same behavior.

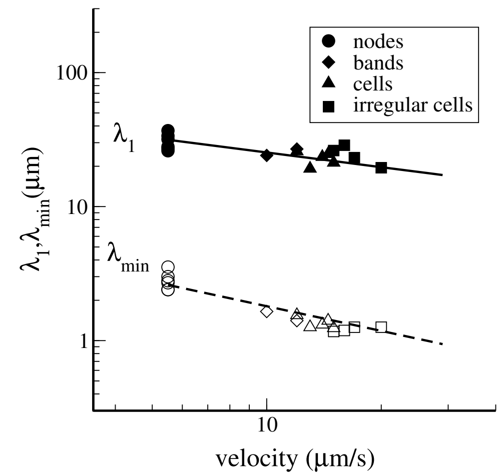


Figure 3: Representation of $\lambda_1$ and $\lambda_{min}$ against growth velocity.

Once defined the primary spacing, depressed zones advances slowly and increases its composition, forming eutectic nodes. However, as it can be seen in Fig. 1, it is usual among nodes, that a secondary level of segregation appears, leaving in the sample a segregation pattern revealed by proper metallography.

The pattern is characterized by a small perturbation during the final growth of two adjacent cells, trapping the last enriched liquid. The $\lambda_{min}$ measured is significantly less than $\lambda_1$. This fact can be seen in In Fig. 3, where $\lambda_1$ and $\lambda_{min}$ are graphically represented against the growth velocity. Notice that the slopes of both $\lambda_1$ and $\lambda_{min}$ are similar, and $\lambda_{min}$ is close numerically to the minimum wavelength that could be unstable, that is $\lambda_0^-$. This fact suggests that though the primary spacing is formed fundamentally by wavelengths close to $\lambda_{\sigma_M}$, when eutectic nodes precipitate, other wavelengths between $\lambda_0^-$ and $\lambda_{\sigma_M}$ could survive. Then it seems to be logical to assume that once a eutectic node is formed, the lateral growth is driven by local solidification conditions, and as a consequence, it may be stable or unstable, depending on the local thermodynamical conditions affecting the local parameter $(G_L/V^*C^*)$, where $V^*$ and $C^*$ are now the effective normal velocity and the effective concentration value at the local S-L interface. These different cases are metallographically detected as a plane segregation wall (stable) or undulated segregation pattern (unstable with $\lambda_{min} \sim \lambda_0^-$).

Once the nodes are fixed, the lateral cellular growth can assume different possibilities, as suggested in Fig. 4:

i. Lateral growth of the adjacent cells are stable: this case corresponds to a bidirectional growth where the interfaces confine an enriched liquid, which reach up the eutectic composition [5, 8]. This situation concludes with a divorced continuous eutectic forming the wall, as can be seen in Fig. 4 a).

ii. One lateral growth is unstable: In this case, a regular segregated pattern appears, showing a planar interface on one side and a rugosity $\lambda_{min}$ on the other. This situation is shown in Fig. 1 a) and b) and Fig. 4 b), and it is the most common case found in the present experiments. This suggests that considering that local solidification conditions define the wavelength $\lambda$ present at S-L interface, the planar interface of one side would grow with $\lambda \tilde{<} \lambda_0^-$, while the undulated S-L interface with a value $\lambda \tilde{>} \lambda_0^-$, defining $\lambda_{min}$.

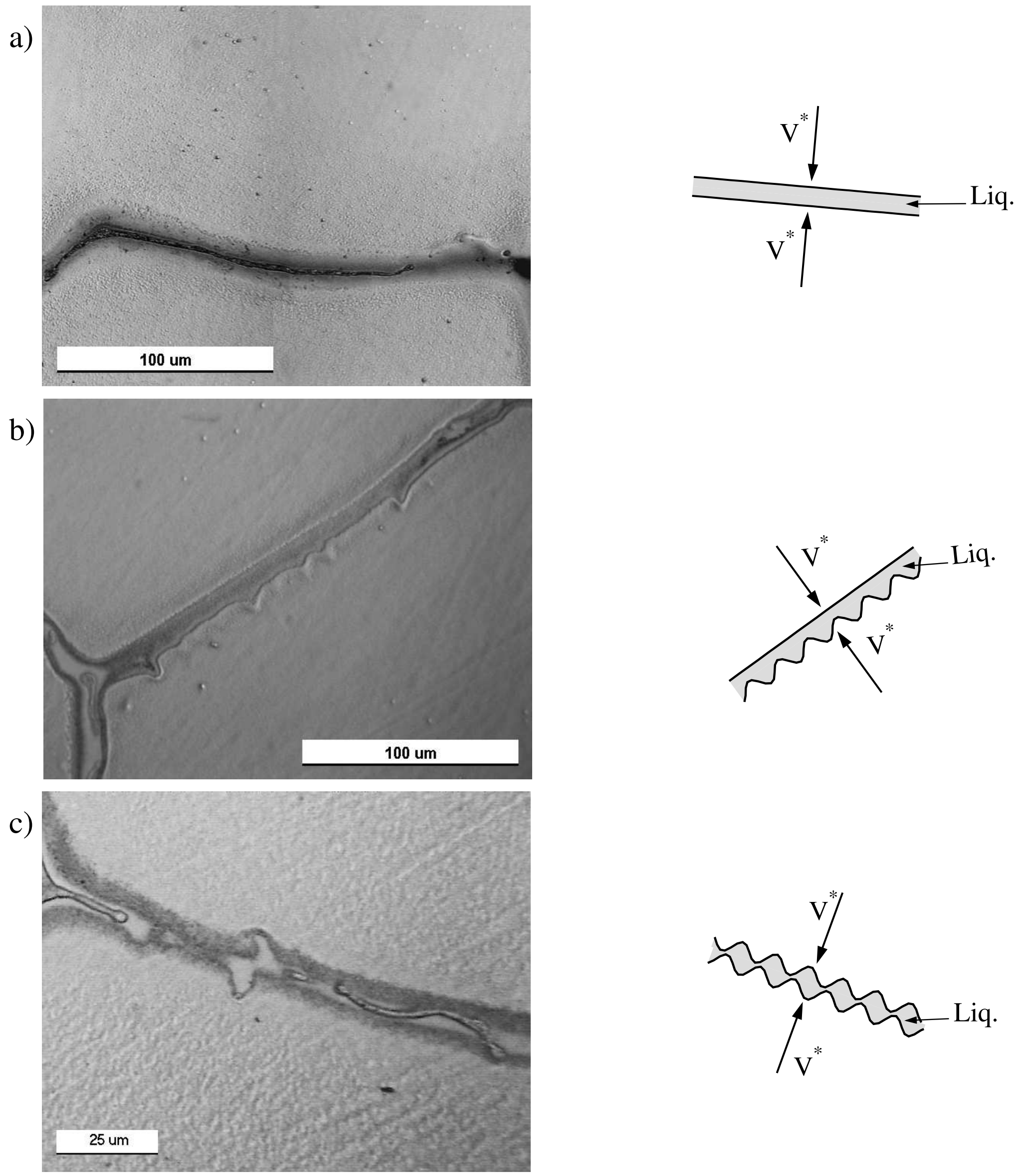


Figure 4: Different cellular wall morphologies and a schematic interpretation of the microstructure. a) lateral of two adjacent cells are stable; b) one of the lateral growth is unstable; c) both lateral growth are unstable.

iii. Both are unstable: given that small undulations are of similar wavelengths from both sides, in this case it is possible to obtain divorced eutectic precipitation in local depressions of the interface. The origin may be a localized final solidification transient and or a solid precipitation during freezing of Cu enriched areas, an effect related to the morphological characteristic of the solvus line of the Al-Cu alloy. Also, a continuous non planar eutectic wall could be found, as in Fig. 4 c), and the origin of the microstructure may be similar to the final solidification transient already discussed in case (i).

## Conclusions

Under our experimental conditions, the evolution of the segregation substructure and the final segregation map for each stage and transitions from (i) to (v), seem to be a result of two superimposed growing mechanism able to be explained qualitatively by the morphological stability theory: i) The evolution from stages (i) to (v) is a consequence of wavelengths of maximum propagation rate as predicted by the theory and the eutectic nodes fixed the local growth, conditioning the evolution of the substructure; ii) The minor instabilities $\lambda_{min}$ associated to the microsegregation of the substructure walls are a result of the lateral solidification of the substructure, with a wavelength close to minimum marginal stability.

Acknowledgment This work was performed at IFIMAT (Instituto de Física de Materiales Tandil) and was supported by CICPBA (Comisión de Investigaciones Científicas de la Provincia de Buenos Aires), CONICET (Consejo Nacional de Investigaciones Científicas y Técnicas) and SeCyT-UNCentro (Secretaría de Ciencia y Técnica de la Universidad Nacional del Centro).

## References

[1] R. F. Sekerka, "Morphological and hydrodinamic instabilities during phase transformations". *Physica D*, **12** (1984) 212–214.

[2] S. R. Coriell, G. B. McFadden, and R. F. Sekerka, "Effect of anisotropic thermal conductivity on the morphological stability of a binary alloy". *J. Crystal Growth*, **100** (1990) 459.

[3] S. R. Coriell and G. B. McFadden (1993) *Morphological Stability*, chap. 12. Handbook of Crystal Growth. D. T. Hurle, 785.

[4] R. Trivedi and W. Kurz, "Solidification microstructures: A conceptual approach". *Acta Metall. Mater.*, **42** (1994) 15–23.

[5] H. Biloni and W. J. Boettinger (1996) Physical Metallurgy, 4 ed. Elsevier Science Publishers, 669–842.

[6] H. Biloni, R. di Bella, and G. F. Bolling, "On microsegregation nodes and cellular solidification substructures in dilute tin alloys". *Trans. Met. Soc. AIME*, **239** (1967) 2012.

[7] W. A. Tiller and J. W. Rutter, "The effect of growth conditions upon the solidification of binary alloy". *Can J. Phys.*, **34** (1956) 96.

[8] B. Chalmers (1964) *Principles of Solidification*. Wiley and Sons, New York.

[9] W. Kurz and D. J. Fisher, "Dendrite growth at the limit of stability: Tip radius and spacing". *Acta Metall.*, **29** (1981) 11–20.

[10] D. J. Wollkind and L. A. Segel, "A non linear stability analysis of the freezing of a dilute binary alloy". *Phil. Trans. R. Soc. London A*, **268** (1970) 351–380.

[11] J. D. Wollkind, R. Sriranganathan, and D. B. Oulton, "Interfacial patterns during plane front alloy solidification". *Physica D*, **12** (1984) 215–240.

[12] O. Fornaro and H. A. Palacio, "Primary spacing evolution during directional solidification of Al-0.5 %Cu". *Scripta Metall. Mater.*, **31** (1994) 1265–1270.

[13] O. Fornaro and H. A. Palacio, "Planar to cellular transition during directionl solidification of Al-0.5 wt.% Cu". *Scripta Mater.*, **36** (1997) 439–445.

[14] O. Fornaro, H. A. Palacio, and H. Biloni, "Subcritical bifurcation from planar to cellular interface in Al-0.5 wt.% Cu directionally solidified". *Mat. Res. Soc*, **481** (1998) 21–26.

[15] R. Trivedi and W. Kurz, "Morphological stability of a planar interface under rapid solidification conditions". *Acta Metall.*, **34** (1986) 1663–1670.

[16] Z. Bi and R. F. Sekerka, "Phase field modeling of shallow cells during directional solidification of a binary alloy". *Journal of Crystal Growth*, **237-239** (2002) 138–143.

[17] S. Cheveigné, C. Guthmann, and M. M. Lebrun, "Cellular instabilities in directional solidification". *J. Physique*, **47** (1986) 2095–2103.

[18] S. de Cheveigné, C. Guthmann, P. Kurowski, E. Vicente, and H. Biloni, "Directional solidification of metallic alloys: The nature of the bifurcation from planar to cellular interface". *J. Crystal Growth*, **92** (1988) 616–628.

[19] W. Boettinger and J. Warren, "Simulation of the cell to plane front transition during directional solidification at high velocity". *J. of Crystal Growth*, **200** (1999) 583–591.